

## Magnetic properties of EuTe-PbTe superlattices

J. Heremans and D. L. Partin

*Department of Physics, General Motors Research Laboratories, Warren, Michigan 48090-9055*

(Received 5 October 1987; revised manuscript received 30 November 1987)

We report the magnetic susceptibility as a function of temperature ( $4 < T < 200$  K) and magnetic field ( $1000 < H < 7000$  Oe) of EuTe/PbTe superlattices grown by molecular-beam epitaxy. Three superlattices were used, consisting of four EuTe monolayers alternating with four PbTe monolayers (EuTe)<sub>4</sub>/(PbTe)<sub>4</sub>, (EuTe)<sub>2</sub>/(PbTe)<sub>6</sub>, and (EuTe)<sub>1</sub>/(PbTe)<sub>3</sub> monolayers. The magnetic field was applied both in the plane of the layers and perpendicularly to it. Only the superlattice with four Eu monolayers shows an antiferromagnetic phase transition, at a nearly isotropic Néel temperature  $T_N = 8.5 \pm 0.7$  K comparable to that of bulk EuTe. In the paramagnetic regime, the susceptibility follows a Curie-Weiss behavior, with an anisotropic Curie-Weiss temperature  $\Theta$ . This was explained with use of molecular-field theory by considering the influence of the strain in the superlattice layers on the Eu-Eu nearest-neighbor and next-nearest-neighbor interactions:  $\Theta$  depends on both, while  $T_N$  depends only on the latter, which is less strain dependent. The (EuTe)<sub>4</sub>/(PbTe)<sub>4</sub> and the (EuTe)<sub>2</sub>/(PbTe)<sub>6</sub> superlattices have roughly the same values for  $\Theta$ , but the latter has no phase transition, presumably because the Eu atoms do not have all six of their nearest neighbors.

### I. INTRODUCTION

Dilute magnetic semiconductors (DMS's) are typically either II-VI compounds such as CdTe or IV-VI compounds such as PbTe, in which some metal ions have been replaced by magnetic ions, like Mn or Eu.<sup>1-4</sup> These investigations conclude that the Eu-Eu exchange effects in Pb-Eu-Te are much weaker than the Mn-Mn interactions in II(Mn)-VI compounds, possibly due to the difference in band structure between PbTe (carrier band extreme at the  $L$  point of the Brillouin zone) and II-VI compounds (extreme at the  $\Gamma$  point). Since by making narrow-period superlattices, it is in principle possible to fold the  $L$  points of the PbTe crystal into the  $\Gamma$  point of a superlattice, we initiated the present study. Also in CdTe-Cd<sub>1-x</sub>Mn<sub>x</sub>Te superlattices<sup>5</sup> there have been deviations reported from the bulk magnetic behavior of DMS's. The present paper describes experiments on samples with too few free electrons to exhibit zone-folding effects, but the effect of strain in the superlattice layers on the magnetic susceptibility is identified.

### II. EXPERIMENTAL

We studied narrow-period EuTe/PbTe superlattices grown along their  $\langle 111 \rangle$  crystallographic orientation. Both EuTe and PbTe grow in the NaCl structure, so that along a  $\langle 111 \rangle$  axis the high-density atomic planes are alternating planes of Eu (or Pb) and Te atoms. Three superlattices were used in this work, which we labeled 1/3, 2/6, and 4/4. The unit cell of a superlattice  $n/m$  was grown to consist of  $n$  monolayers of Eu atoms alternating with  $n$  monolayers of Te atoms, followed by  $m$  monolayers of Pb atoms alternating with  $m$  monolayers of Te atoms. The samples were grown by molecular-beam epitaxy<sup>6</sup> starting from a freshly cleaved BaF<sub>2</sub>  $\langle 111 \rangle$  surface.

On that surface a PbTe buffer layer was grown followed by the EuTe/PbTe superlattice. The detailed properties of the various layers are given in Table I. Because of defects at the BaF<sub>2</sub>/PbTe interface, an areal hole density of  $\sim 10^{13}$  cm<sup>2</sup> (Ref. 7) is normally observed at that interface, which would correspond to hole densities ranging from  $4 \times 10^{16}$  to  $3 \times 10^{17}$  cm<sup>-3</sup> in our buffer layers. But the samples used here were essentially insulating, and no numbers for the real carrier density could be obtained. Detailed high-resolution transmission-electron-microscopy studies were carried out<sup>8</sup> on PbTe/PbEuSeTe superlattices which were grown under similar conditions and are similar in nature. They show that the layer boundaries are sharp within two atom planes.

The magnetic susceptibility was measured in the temperature range  $4 < T < 200$  K for fields  $1 < H < 7$  kOe using a S.H.E. Corp. SQUID (superconducting quantum-interference device) magnetometer. Each sample was measured in two configurations: with the magnetic field parallel and perpendicular to the film plane. Two different sample holders were used. In each case we measured the susceptibility of the empty sample holders separately, because they had a slight temperature dependence, and subtracted the susceptibility of the holder from the data taken on the samples. The samples were weighted, with an accuracy of 1 part in  $10^5$ , and the film area measured, with an accuracy of  $\sim 10\%$ . From this we deduced the amount of BaF<sub>2</sub> and PbTe buffer in each sample, and since it was shown that the susceptibility of epitaxial PbTe and BaF<sub>2</sub> had almost no temperature dependence,<sup>2</sup> we again subtracted these diamagnetic contributions to the measured susceptibility. We analyzed our data in terms of a Curie-Weiss law with three parameters,  $C_e$  the experimental Curie constant,  $\Theta$  the Curie-Weiss temperature and in the fit we also allowed for a temperature-independent contribution  $\chi_d$  to the total measured susceptibility  $\chi_m$ :

$$\chi_m = \chi_d + \frac{C_e}{T - \Theta} \quad (1)$$

We fitted data taken at 1 kOe field over the whole temperature range.  $\chi_d$  was  $9 \pm 5\%$  of  $\chi_m$  at 200 K, illustrating the reliability of the background-subtraction procedure. In Fig. 1 we show the temperature dependence of the susceptibility

$$\chi = \frac{C_e}{T - \Theta} \quad (2)$$

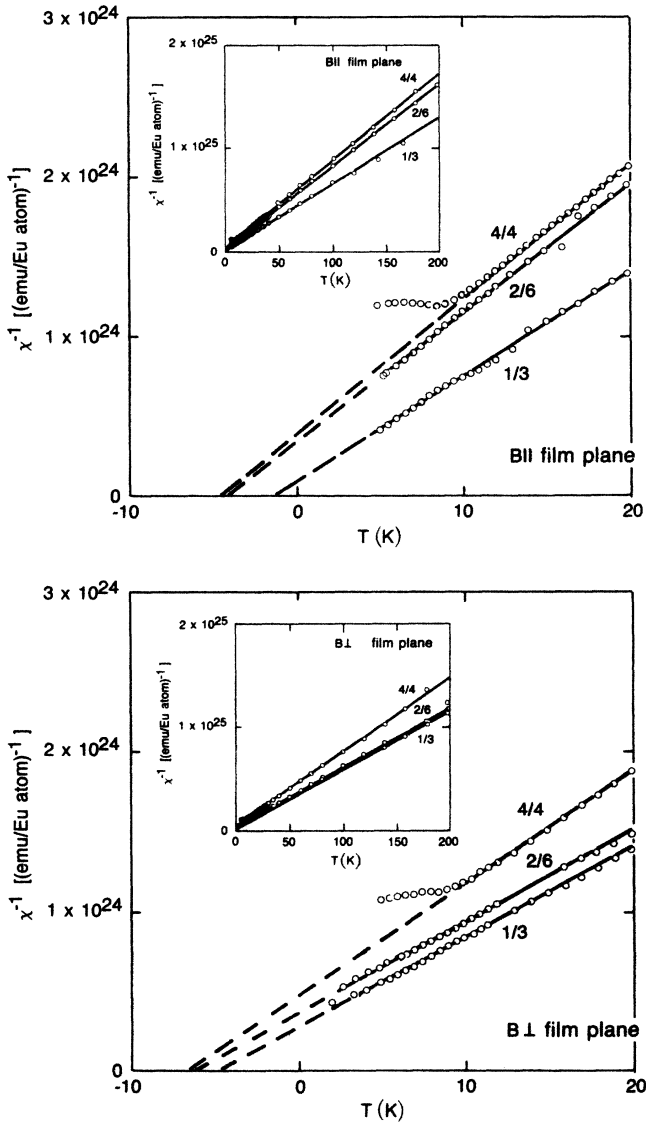


FIG. 1. The inverse susceptibility  $\chi^{-1}$  as a function of temperature for the three superlattices studied. The inset shows the high-temperature ranges. The top frame is for the external magnetic field applied in a direction parallel to the superlattice planes, the bottom frame for the field perpendicular to them, i.e., along a  $\langle 111 \rangle$  axis. The points are the experimental data; the lines show the fit to the Curie-Weiss law in the paramagnetic temperature range. The fitted Curie-Weiss temperature  $\Theta$  and constant  $C_e$ , are reported in Table II.

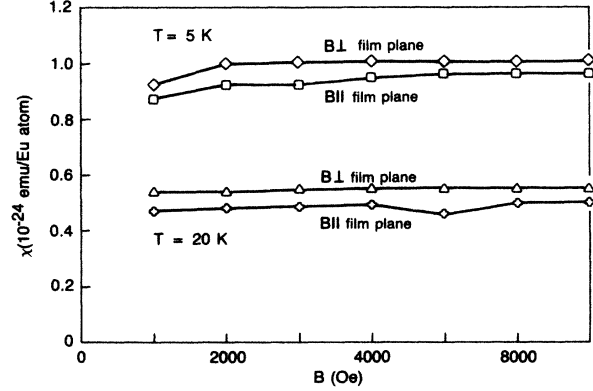


FIG. 2. The magnetic field dependence of the susceptibility at two temperatures (5 and 20 K) of sample 4/4, which has an antiferromagnetic transition at  $T_N = 8.5$  K. The field is applied in the directions shown with respect to the superlattice planes.

for the three samples studied with an applied magnetic field of 1 kOe (roughly half the effective molecular field  $k_B T_N / 7\mu_B$  of EuTe) applied parallel and perpendicularly to the superlattice planes. Only sample 4/4 shows an antiferromagnetic phase transition below  $T_N = 8.5 \pm 0.7$  K, a temperature quite close to that of bulk EuTe [ $9.58 \pm 0.1$  K (Ref. 9)].

In Fig. 2 we show the magnetic-field dependence of the susceptibility of sample 4/4 at temperatures both above and below  $T_N$ , in both field directions. In the field and temperature range available for this experiment,  $\chi$  is constant, which is compatible with the fact that there are very few free carriers in the layers which could cause a spontaneous magnetic moment.<sup>10</sup>

### III. DISCUSSION

The temperature dependence of the susceptibility (Fig. 1) in the paramagnetic region was analyzed in terms of a Curie law [Eq. (1) and (2)], and the experimentally determined Curie constants  $C_e$  and temperature  $\Theta$  are shown in Table II. Also reported is the transition temperature  $T_N$  (the abscissa value of  $T$  at which  $\chi^{-1}$  in Fig. 1 is minimal) observed on sample 4/4.

In molecular-field theory, as applied to Eu chalcogenides, two coupling terms play a significant role: nearest-neighbor interactions ( $J_1$ ) and next-nearest-

TABLE I. Growth properties of the superlattices used: the thickness of the PbTe buffer layer, the number of periods in the superlattice, and the thickness of each EuTe and PbTe layer within one period, in Å and in monolayers.

	Sample		
	1/3	2/6	4/4
Buffer thickness ( $\mu\text{m}$ )	2.4	0.5	0.4
Number of periods	500	400	100
Thickness of EuTe/PbTe			
(Å)	4.23/13.38	7.83/23.8	15.2/14.9
(monolayers)	1.11/3.59	2.06/6.38	4.0/4.0

TABLE II. Magnetic parameters of the superlattices with the applied magnetic field parallel and perpendicular to the lattice planes.  $\Theta$  is the Curie-Weiss temperature and  $C_e$  the Curie-Weiss constant obtained from the data in the paramagnetic range,  $T_N$  the antiferromagnetic transition temperature, and  $\bar{a}$  the average lattice parameter of the strained superlattice.

	Samples					
	1/3		2/6		4/4	
Magnetic field	Parallel	Perpendicular	Parallel	Perpendicular	Parallel	Perpendicular
$\Theta$ (K)	$-1.36 \pm 0.11$	$-4.74 \pm 0.14$	$-4.06 \pm 0.10$	$-6.26 \pm 0.15$	$-4.46 \pm 0.10$	$-6.37 \pm 0.18$
$C_e$ ( $10^{-23}$ emu/Eu-atom)	$1.54 \pm 0.11$	$1.75 \pm 0.12$	$1.25 \pm 0.09$	$1.73 \pm 0.11$	$1.18 \pm 0.09$	$1.40 \pm 0.10$
$T_N$ (K)					$8.5 \pm 0.5$	$8.5 \pm 0.7$
$\bar{a}$ (Å)	6.486	6.585	6.487	6.585	6.516	6.585

neighbor interactions ( $J_2$ ) (Refs. 9 and 11). The susceptibility in the paramagnetic region is

$$\chi_p = \frac{C}{T - \Theta}, \quad (3)$$

$$C = N_{\text{Eu}} g^2 \mu_B^2 S(S+1) \frac{1}{3k_B} = 1.30 \times 10^{-23} \frac{\text{emu}}{\text{Eu atom}}, \quad (4)$$

$$\Theta = \frac{2}{3} S(S+1)(12J_1 + 6J_2) = 126J_1 + 63J_2, \quad (5)$$

while the Néel temperature  $T_N$  for EuTe is

$$T_N = \frac{2}{3} S(S+1)(-6J_2) = -63J_2. \quad (6)$$

In these equations,  $N_{\text{Eu}}$  is the density of Eu atoms,  $g=2$ ,  $S=\frac{7}{2}$ .

The fact that we see anisotropy in the Curie-Weiss temperature  $\Theta$  of all samples is a strong indication that the effect is due to strain. The lattice constant  $a_{\text{Eu}} = 6.585 \text{ \AA}$  (Ref. 10) of EuTe is 1.9% larger than that  $a_{\text{Pb}} = 6.462 \text{ \AA}$  (Ref. 12) of PbTe, so the EuTe is under compression. Ignoring the influence of the BaF<sub>2</sub> substrate and the PbTe buffer layer because the superlattices are thick, we can estimate that the average lattice constant<sup>13</sup> in the  $\langle 111 \rangle$  plane is

$$\frac{\bar{a}}{\sqrt{3}} = \frac{(C_{11\text{Eu}} + 2C_{12\text{Eu}})t_{\text{Eu}}a_{\text{Eu}} + (C_{11\text{Pb}} + 2C_{12\text{Pb}})t_{\text{Pb}}a_{\text{Pb}}}{(C_{11\text{Eu}} + 2C_{12\text{Eu}})t_{\text{Eu}} + (C_{11\text{Pb}} + 2C_{12\text{Pb}})t_{\text{Pb}}} / \sqrt{3}, \quad (7)$$

where  $C_{ij}$  are the elastic stiffnesses,  $t$  the thicknesses, and  $a$  the lattice parameters. The subscript Eu and Pb refer, respectively, to the EuTe and PbTe layers. For the EuTe layer the value of the lattice parameter along the  $\langle 111 \rangle$  axis, of course, remains  $a_{\text{Eu}}/\sqrt{3} = 6.585/\sqrt{3} \text{ \AA}$ .

Using the stiffnesses reported by Wachter<sup>10</sup> for EuTe and Lucovsky, Martin, and Burstein<sup>14</sup> for PbTe, and the layer thicknesses of Table I, we can calculate the values of  $\bar{a}$  and report them in Table II. This elastic model assumes that there are no dislocations, and that is consistent with the observations in Ref. 8. We can now estimate the influence of this strain using known data on the dependence of the magnetic parameters ( $T_N$ ,  $\Theta$ , or  $J_1, J_2$ ) on the lattice constant, mainly through measurements on other Eu chalcogenides as suggested in Refs. 11 and 9. There have been a number of refinements in the experimental determination of  $J_1$  and  $J_2$ , and in Fig. 3 we use the values summarized by Wachter.<sup>10</sup> In Fig. 3 we plot as a solid curve the value of  $126J_1 + 63J_2$  [=  $\Theta$ , Eq. (5)] as function of the lattice parameter of the different Eu chalcogenides. We also plot as a dashed curve the value of  $-63J_2$  [=  $T_N$ , Eq. (6)] interpolating between EuTe and EuO,<sup>10</sup> even though the points for EuSe and EuS do not fit very well. We then add our experimental data points (the vertical bars): they are the values we obtain for the Néel temperature of sample 4/4 and for the Curie-Weiss temperature of samples 4/4 and 2/6, plotted as a function

of the relevant lattice parameter as given in Table II. The fit illustrates that strain is the probable cause of the variations in  $\Theta$ , and the relative anisotropy of  $T_N$  is consistent with the insensitivity of  $J_2$  to the lattice constant, although this property is not well understood.<sup>15</sup>

Since the next-nearest-neighbor interaction ( $J_2$ ) is driving the antiferromagnetic phase transition, it is no surprise that samples 1/3 and 2/6 show no transition, at least for the field perpendicular to the planes. For sample 1/3,  $|\Theta|$  is smaller than what would be predicted by Fig. 3, probably because the EuTe layer itself may no longer be continuous. Reference 8 shows that PbTe/Pb<sub>1-x</sub>Eu<sub>x</sub>Se<sub>y</sub>Te<sub>1-y</sub> heterojunctions had an interface roughness of about two lattice planes. A Curie-Weiss temperature  $\Theta$  of  $-4.6 \text{ K}$  was reported<sup>2</sup> on a random Pb<sub>0.684</sub>Eu<sub>0.316</sub>Te alloy, which compares with the results on sample 1/3. Sample 2/6 has the same Eu concentration as sample 1/3, and some amount of intermixing probably took place in sample 2/6 too. However, the values of  $\Theta$  and  $T_N$  of sample 2/6 are closer to that of sample 4/4, i.e., strained EuTe, indicating that a large fraction of the EuTe is in continuous planes. It is hence suggested that the absence of magnetic ordering in sample 2/6 could be related to the two-dimensional nature of the EuTe layers, in which Eu atoms do not have all six of their nearest neighbors as in a three-dimensional (3D) lattice.

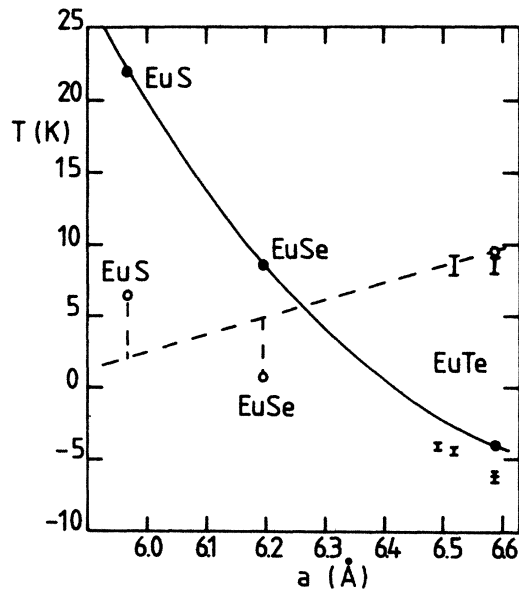


FIG. 3. The Curie-Weiss temperatures  $\Theta$  (solid dots connected by a solid line) and Néel temperatures  $T_N$  (open dots, dashed line) calculated using Eqs. (5) and (6) for bulk Eu chalcogenides as function of their lattice parameters. The vertical error bars are our experimental data points for the Néel temperatures of sample 4/4 and the Curie-Weiss temperatures of samples 2/6 and 4/4 plotted as function of their strained lattice parameter as given in Table II.

The value of the experimental Curie constants  $C_e$  should be compared to the calculated value of  $1.3 \times 10^{-23}$  emu/atom [Eq. (4)]. The main source of uncertainty is in the measurement of the area of the film. The agreement

between theory and experiment is about as good (20%) as it was for random  $\text{Pb}_{1-x}\text{Eu}_x\text{Te}$  alloys,<sup>2</sup> although we may have an indication that  $C_e$  is anisotropic in sample 2/6.

#### IV. CONCLUSIONS

We have studied the magnetic susceptibility of EuTe/PbTe small-period superlattices. The antiferromagnetic phase transition that occurs in bulk EuTe can indeed be observed in superlattices in which each Eu atom has all its six next-nearest neighbors, and not when that is not the case, either through intermixing or because EuTe is in layers only two lattice planes thick, with PbTe boundaries. The Néel temperature  $T_N$  is rather isotropic, while the Curie-Weiss temperature  $\Theta$  obtained from extrapolating the inverse susceptibility in the paramagnetic temperature range depends on the direction of the applied magnetic field. This is consistent with the present of  $\sim 1\%$  strain in the superlattice planes, which influences  $\Theta$ . There were very few free carriers in these superlattices, precluding the study of the possible influence on their magnetic properties of zone folding of the Fermi surfaces normally located at the  $L$  points of the Brillouin zone of PbTe to the  $\Gamma$  points of the superlattices.

#### ACKNOWLEDGMENTS

We would like to thank Lauren Hill and Prof. J. Dye for their help in making the measurements with the SQUID magnetometer at Michigan State University, C. M. Thrush for help in sample growth, and Dr. G. Dresselhaus, and Dr. W. Goltos, and Professor A. V. Nurmikko for helpful discussions.

<sup>1</sup>J. K. Furdyna, *J. Appl. Phys.* **53**, 7637 (1982).

<sup>2</sup>G. Braunstein, G. Dresselhaus, J. Heremans, and D. L. Partin, *Phys. Rev. B* **35**, 1969 (1987).

<sup>3</sup>W. C. Goltos, A. V. Nurmikko, and D. L. Partin, *Mater. Res. Soc. Symp. Proc.* **89**, 299 (1987).

<sup>4</sup>J. R. Anderson and M. Gorska, *Solid State Commun.* **52**, 601 (1984); M. Bartkowski, A. H. Reddoch, D. L. Williams, G. Lamarche, and Z. Korcak, *Solid State Commun.* **57**, 185 (1986), and references therein.

<sup>5</sup>D. D. Awschalom, S. von Molnar, J. Yoshino, H. Munekata, and L. L. Chang, *Bull. Am. Phys. Soc.* **32**, 918 (1987).

<sup>6</sup>D. L. Partin, *J. Electron. Mater.* **13**, 493 (1984).

<sup>7</sup>D. L. Partin, J. Heremans, C. H. Olk, C. M. Thrush, and L. Green (unpublished).

<sup>8</sup>L. Salamanca-Young, D. L. Partin, J. Heremans, and E. M.

Dresselhaus, *Mater. Res. Soc. Symp. Proc.* **77**, 199 (1987).

<sup>9</sup>P. Schwob, *Physics of Condensed Matter* (Springer-Verlag, Berlin, 1969), Vol. 10, p. 186.

<sup>10</sup>P. Wachter, in *Handbook on the Physics and Chemistry of the Rare Earths*, edited by K. A. Gschneidner, Jr. and L. Eyring (North-Holland, Amsterdam, 1979), p. 507.

<sup>11</sup>T. R. McGuire, B. E. Argyle, M. W. Shafer, and J. S. Smart, *J. Appl. Phys.* **34**, 1345 (1963).

<sup>12</sup>R. Dalven, *Infrared Phys.* **9**, 141 (1969).

<sup>13</sup>A. Banerjee and J. R. Smith, *Phys. Rev. B* **35**, 5413 (1987).

<sup>14</sup>G. Lucovsky, R. M. Matrin, and E. Burstein, in *Physics of IV-VI Compounds and Alloys*, edited by S. Rabii (Gordon and Breach, London, 1974), p. 93.

<sup>15</sup>L. Liu, *Solid State Commun.* **46**, 83 (1983).